Civil and Architectural Engineering

Influence of Fire-Flame Duration and Temperature on the Behavior of Reinforced Concrete Beam Containing Water Absorption Polymer Sphere; Numerical Investigation

Nibras Farooq Hussen*	**Shatha Dheyaa Mohammed**
MSc student	Assistant Professor, PhD
Department of Civil Engineering	Department of Civil Engineering
College of Engineering	College of Engineering
University of Baghdad,	University of Baghdad,
Baghdad-Iraq	Baghdad-Iraq
n.hussen1901m@coeng.uobaghdad.edu.iq	shatha.dh@coeng.uobaghdad.edu.iq

ABSTRACT

One of the most important parameters determining structural members' durability and strength is the fire flame's influence and hazard. Some engineers have advocated using advanced analytical models to predict fire spread impact within a compartment and considering finite element models of structural components to estimate the temperatures within a component using heat transfer analysis. This paper presented a numerical simulation for a reinforced concrete beam's structural response in a case containing Water Absorbing Polymer Spheres (WAPS) subjected to fire flame effect. The commercial finite element package ABAQUS was considered. The relevant geometrical and material parameters of the reinforced concrete beam model at elevated temperature are first suggested as a numerical model. After that, the suggested numerical model was validated against the experimental tests conducted in this study. The validated numerical model was used to conduct a parametric study to investigate the effects of two important parameters on the structural behavior after being exposed to fire flame. The effect of burning temperatures (500, 600, and 700) °C, as well as the influence of fire duration (1 and 2) hours, were included. The experimental program validation requirement comprised four self-compacted reinforced concrete beams each of the same geometric layout (150x200x1500) mm, reinforcing details, and compressive strength (fc'=50 MPa). Four percentages of (WAPS) were considered (0, 1, 2, and 3)%. The specimens were exposed to a fire flame with a steady-state temperature (500°C), a rising rate compatible with ASTM-E119, a one-hour duration, and a sudden cooling procedure. A static (two-point) load was applied to the burned beams.

Through the assessed numerical model, the numerical analysis offered by the WAPS ratio effect was carried out for the reinforced concrete beam under the effect of static load. The findings revealed that the WAPS ratio substantially impacted structural behavior. The numerical model's results were in reasonable agreement with the experimental results. Concerning the fire exposure duration (two hours) at 500 $^{\circ}$C, the specimens containing a ratio (3%) of WAPS improved the ultimate load and the ultimate deflection by about (46.63 and 72.24)%, respectively. The highest percentage variation of the absorbed energy at failure load was also detected in the ratio (3%) to be (139.43) %. As for the hardening concrete properties (compressive strength, splitting tensile strength, and modulus of elasticity), the residual strength was (61.06, 48.87, and 32.00)%, respectively. Regarding the steady-state burning temperature (500, 600, and 700)$^{\circ}$C for a one-hour duration, the specimens with a ratio of (3%) WAPS improved the ultimate load by about (40.70, 62.00, and 40.76)%, respectively, corresponding to zero percentage of WAPS. The residual compressive strength, splitting tensile strength, and modulus of elasticity were (72.40, 56.12, and 43.78)%, (74.36, 56.50, and 44.79)%, and (45.23, 36.57, and 28.94)%, respectively.

Keywords: WAPS, Finite Element Methods, R.C.B., Elevated Temperature, Fire Duration.

تأثير مدة اللهب ودرجة الحرارة على سلوك عارضة الخرسانة المسلحة التي تحتوي على كرة بوليمر لامتصاص الماء ؛ التحقيق العددي

ا.م.د. شذى ضياء محمد	* نبراس فاروق حسين
قسم الهندسة المدنية- كلية الهندسة – جامعة بغداد	قسم الهندسة المدنية- كلية الهندسة – جامعة بغداد

الخلاصة

من أهم العوامل التي تحدد متانة وقوة العناصر الهيكلية هو تأثير ومخاطر اللهب الناري. دعا بعض المهندسين إلى استخدام النماذج التحليلية المتقدمة للتنبؤ بتأثير انتشار الحريق داخل مقصورة ، بالإضافة إلى النظر في نماذج العناصر المحدودة للمكونات الهيكلية لتقدير درجات الحرارة داخل أحد المكونات باستخدام تحليل نقل الحرارة. يقدم هذا البحث محاكاة عددية للاستجابة الهيكلية للحزمة الخرسانية المسلحة في حالة تحتوي على كريات بوليمر ماصة للماء (WAPS) ومعرضة لتأثير اللهب. تم النظر في حزمة العناصر المحدودة التجارية. ABAQUS تم اقتراح المعلمات الهندسية والمادية ذات الصلة لنموذج عارضة الخرسانة المسلحة عند درجة حرارة مرتفعة كنموذج عددي. بعد ذلك تم التحقق من صحة النموذج العددي المقترح مقابل الاختبارات التجريبية التي أجريت في هذه الدراسة. تم استخدام النموذج العددي الذي تم التحقق منه لإجراء دراسة بارامترية للتحقق من تأثير معلمتين هامتين على السلوك الإنشائي بعد التعرض لهب النار . تم تضمين تأثير درجات حرارة الاحتراق (500 ، 600 ، 700) درجة مئوية ، وتأثير مدة الحريق (1 و 2) ساعة. يتكون البرنامج التجريبي ، متطلبات التحقق من الصحة ، من أربعة عوارض خرسانية مسلحة مضغوطة ذاتيًا ، كل منها من نفس التصميم الهندسي (150 × 200 × 1500) ملم ، وتفاصيل التعزيز ، وقوة الضغط (fc' = 50) ميجا باسكال . تم اعتبار أربعة نسب من WAPS (0 ، 1 ، 2 ، 3)٪. تعرضت العينات للهب حريق بدرجة حرارة ثابتة (500 درجة مئوية) ، ومعدل ارتفاع متوافق مع ASTM−E119 ، ومدة ساعة واحدة ، وإجراء تبريد مفاجئ. تم تطبيق حمل ثابت (نقطتين) على الحزم المحترقة .كانت نتائج النموذج العددي متوافقة بشكل معقول مع النتائج

التجريبية. من خلال النموذج العددي المقدر ، تم إجراء التحليل العددي المقدم من تأثير نسبة WAPS لحزمة الخرسانة المسلحة تحت تأثير الحمل الساكن. كشفت النتائج أن نسبة WAPS كان لها تأثير كبير على السلوك الهيكلي. فيما يتعلق بمدة التعرض للحريق (ساعتان) عند 500 درجة مئوية ، فإن العينات المحتوية على نسبة (3٪) من WAPS حسنت الحمل النهائي والانحراف النهائي بحوالي (46.63 و 72.24)٪ على التوالي. كما تم الكشف عن أعلى نسبة تغير في الطاقة الممتصة عند حمل الفشل بنسبة (3٪) لتكون (139.43)٪. أما بالنسبة لخواص الخرسانة المتصلبة (مقاومة الانضغاط ، مقاومة الشد الانشقاقي ، ومعامل المرونة) فكانت المقاومة المتبقية (61.06 ، 48.87 ، 32.00)٪ على التوالي. فيما يتعلق بدرجة حرارة الاحتراق في الحالة المستقرة (500 و 600 و 700) درجة مئوية لمدة ساعة واحدة ، فإن العينات بنسبة (3) ٪ WAPS حسنت الحمل النهائي بحوالي (40.70 و 62.00 و 40.76) ٪ ، على التوالي ، المقابلة لنسبة صفر من WAPS. كانت مقاومة الانضغاط المتبقية وقوة الشد الانشقاقية ومعامل المرونة (72.40 و 56.12 و 43.78)٪ و (74.36 و 56.50 و 44.79)٪ و (45.23 و 36.57 و 28.94)٪ على التوالي.

الكلمات الرئيسية: WAPS, طرق العناصر المحدودة , .R.C.B, درجات الحرارة المرتفعة , مدة الحريق.

1. INTRODUCTION

Concrete has intrinsic fire resistance, which is one of its advantages over other construction materials; yet, concrete structures must still be constructed for fire impacts. Even if the strength and modulus of elasticity of concrete and steel reinforcement diminish as the temperature rises, structural components must still be able to bear dead and live loads without collapsing. Furthermore, fully formed fires cause structural components to expand, resulting in loads and strains that must be resisted. Building code standards for fire resistance are occasionally disregarded in construction, which can lead to costly blunders.

Fire-induced temperature is one of the most extreme stress circumstances that any concrete structure may face over its service life. The higher the temperature, the more likely the concrete's mechanical characteristics will deteriorate, leading to progressive collapse and disintegration of the entire building. For example, the fall of the World Trade Center (WTC) in 2002 was mostly caused by the elevated temperature created by the fire that followed the explosions. Since then, the engineering community has become more conscious of the need to include elevated temperature's influence in structural member design techniques. As a result, over the last two decades, many experimental research investigations on the influence of high temperature on the behavior of concrete members have been done. However, due to the complexity of the problem, numerical studies on RC beam members in the fire have been published. (**Yue et al., 2008**) used the finite element software ABAQUS to conduct numerical simulations to investigate the fireproof behavior of simply supported RC beams enhanced with stranded mesh and polymer mortar (SMPM). The thermal and mechanical properties of concrete are adopted according to (**Eurocode 4, 2005**) and others derived from earlier research investigations, and temperature and displacement analysis are thoroughly considered. The numerical findings show that ABAQUS can reasonably simulate the coupling of displacement and temperature fields. (**Gao et al., 2013**) provided a three-dimensional FE model for predicting RC beams' thermal and mechanical behavior at high

temperatures. The mechanical behavior of concrete was modeled using a concrete damage plasticity constitutive model **(Karlsson and Sorensen, 2008). (Eurocode 2, 2004 and Eurocode 3, 2011)** were used to determine the stress-strain relationship and the thermal characteristics of steel and concrete at extreme temperatures. Furthermore, the concrete reduction factors at elevated temperatures were calculated using experimental data from earlier research investigations, and the steel reduction factors were calculated using **Eurocode 3, 2011)**. The results suggest that including steel to concrete interfacial behavior improves the accuracy of deflection predictions for RC beams exposed to fire. In their numerical investigation, (Ozbolt et al., 2013) built a three-dimensional finite element model to evaluate the response of simply supported RC beams made of crushed stone aggregate. Under increased temperatures up to 300ºC, the **(ISO 834., 1999)** standard fire curve was applied, followed by mechanical loading. The analysis was carried out using the ABAQUS thermal and mechanical procedures. **(Eurocode 2, 2004 and Eurocode 3, 2011)** were used to determine the thermal characteristics of steel and concrete. The results showed that the numerical modeling technique used to anticipate the behavior of the RC beam under fire and the mechanical strain was successful. Furthermore, the 3D thermo-mechanical model used is a useful numerical tool for predicting the behavior of RC structures subjected to high temperatures in a realistic manner. **(Izzat et al., 2012)** conducted an experimental test to investigate the behaviour of a one-way reinforced self-compacted concrete (SCC) slab under the fire flame effect. It was found that the residual flexural strength of the gradually cooled tested slabs is (81.5, 75, and 62.3) % for fire temperatures of (300, 500, and 700) °C, respectively. **(Izzat, 2015)** conducted an experimental test to investigate the behaviour of CFRP wrapping jackets used for retrofitting twelve square reinforced concrete column specimens damaged by exposure to fire flame at different temperatures of (300, 500, and 700) ºC, except for two specimens that were not burned. The ultimate load capacity of each retrofitted specimen was increased by about 16, 34, and 44 percent compared to non-retrofitting burned specimens at (300, 500, and 700)ºC, respectively, and cooled gradually. In contrast, this increase was (44 and 111)% for specimens burned at (500 and 700)ºC, respectively, but cooled suddenly. (**El-Tayeb et al., 2017)** used the FE software ABAQUS to conduct a numerical analysis of the reaction of RC beams and frames under the effect of thermal loads in the same environment. The material nonlinearity, including cracking behavior, was considered while modeling the beams and frames, and temperature gradients were considered linear, nonlinear, and uniform. The findings show that the behavior of beams and frames is mainly influenced by the temperature gradient's trend (i.e., linear or nonlinear). As a result, it was suggested that the nonlinear temperature gradient be used in the analysis.

2. NUMERICAL ANALYSIS

Numerical analysis considering the finite element method was adopted. The finite element method involves a series of processes that begin with the definition of defined elements, the addition of actual constants to each element, the materials model, key points, lines, areas, and then volume to create the whole geometry of the model. Nodal, element solutions are accessible in most (FEA) software to provide the entire solution of the problem, making it easy to calculate any unknown parameter and display it graphically **(D. L. Logan., 2012)**.

FEM requires little training and versatile computer programs; therefore, it has become more popular for tackling various practical issues **(N.-H. Kim., 2014).**

Over the last three decades, substantial advancements in computer-aided and finite element techniques provided an economical solution have made many common 3D structural studies. FEM is used in ABAQUS, a set of engineering simulation programs **(User's Guide., 2014).**

The finite element software ABAQUS/CAE 6.14.1/2019 was used to explore the overall behavior and analysis of reinforced concrete beams containing WAPS and subjected to fire flame. It can address a wide range of problems, from simple linear analysis to the most difficult nonlinear simulations **(Abacus 6.10., 2020).**

Three parts have to be generated for the modeling to be completed. The tetrahedral element was used to model the beam in the first part. The steel reinforcement modeling, which was modeled in a 3D process, was the second part. The third part presented steel support generation, modeled as a 3D-solid object. **Fig. (1) to (3)** show the details of these components.
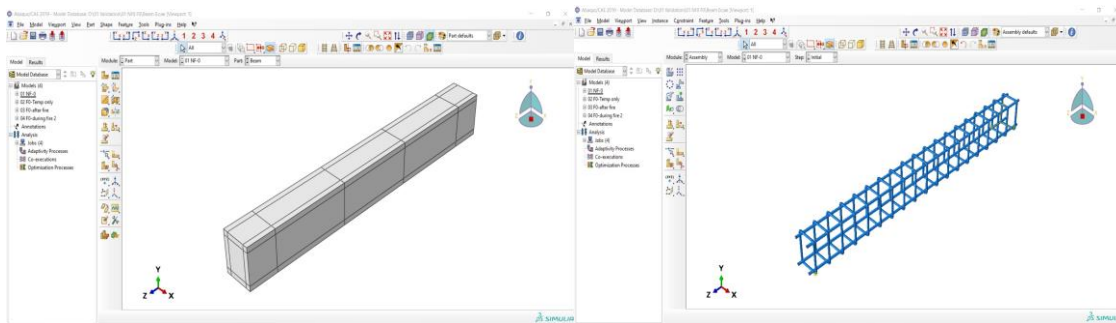
Figure 1. Volume Part of the Concrete Beam.   **Figure 2.** (3D) Parts of the Steel Reinforcement.
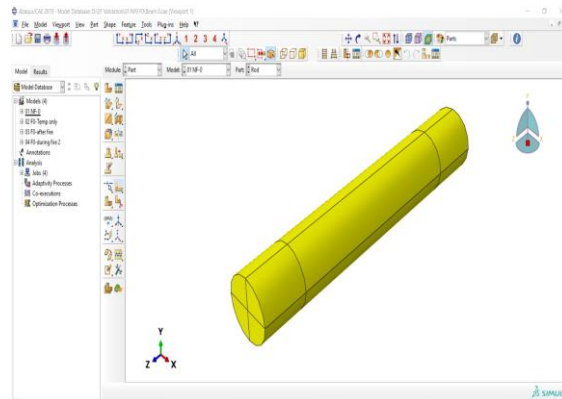
Figure 3. (3D) Parts of the Steel Rod.

The material properties were determined once the specimen parts were created, and appropriate interaction ways between all of the specimen's components were chosen. As indicated in **Fig. (4),** an assembly module method was suggested to perform the acquired model geometry by creating part instances.
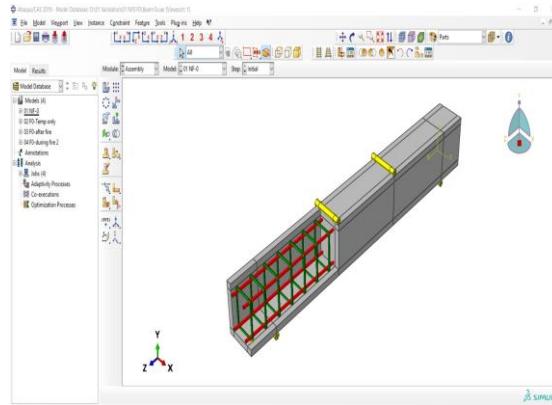
Figure 4. Model Assembly in ABAQUS.

Models were subjected to a two-phase loading technique. The specimen was subjected to a fire concurrently with the effect of a uniform constant equivalent dead load in the first mode. Thus, a uniform pressure load was supplied to the specimen's top surface at about ($10.5 \ kN/m^2$) to imitate the equivalent dead load during the fire exposure duration, **Fig. (5)**. The models were next tested using (the flexural load test), which is the second phase of the test procedure. As a result, applied displacement was all specimens shown in **Fig. (6)**.
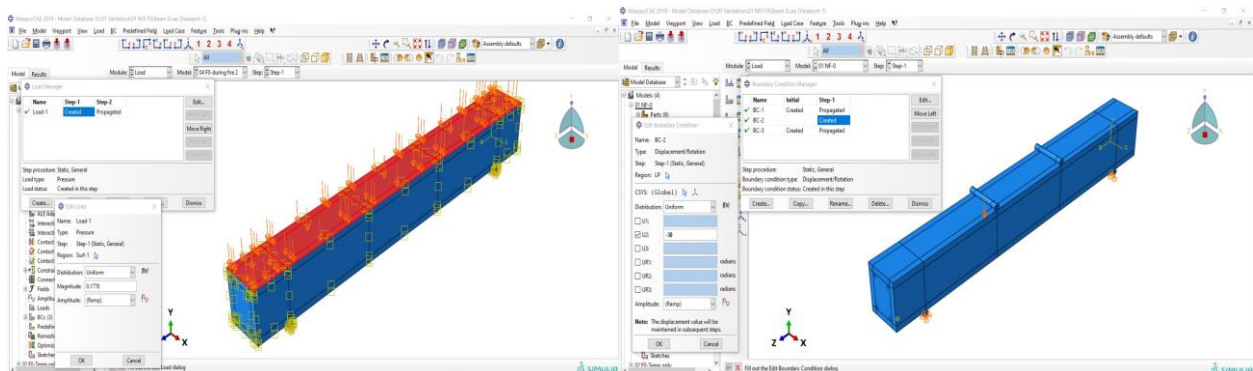
Figure 5. Service Load Application at Burning Stage. **Figure 6.** Displacement control application.

Utilized embedded region limitations to combine two surfaces during a simulation for the burned specimens, every node on the surface is compelled to have the same motion as the point on the master surface to which it is closest with a frictionless contact property. The formulation of connecting interaction-states in the model is shown in **Fig. (7)**. As illustrated in **Fig. (8)**, the surface film constraint in ABAQUS/Explicit was utilized to simulate the fire effect on beam surfaces.
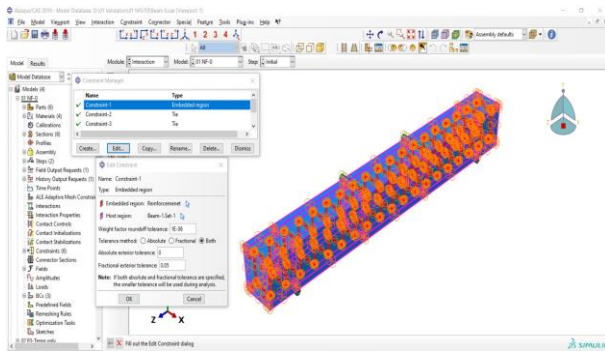
Figure7. Formulation of connecting
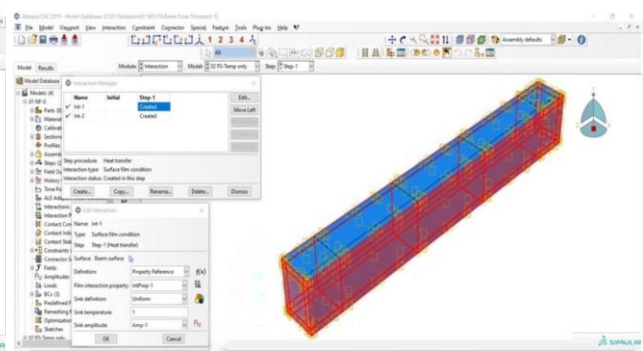
Figure 8. Interaction for the Elevated Temperature.

interaction -states in the model.

The chosen elements in the ABAQUS software contain appropriate integration rules based on the model's experimental response. To evaluate the mesh sensitivity of the FEA model, four different mesh sizes (20 mm, 25 mm, 30 mm, and 35 mm) were used in the study of the specimen. The difference between the experimental ultimate load results and the numerical ultimate load values derived from each of the four mesh sizes was calculated. The mesh size of (25 mm) was determined to provide relatively reliable findings; hence it was used in this study, as indicated in **Fig. (9) to (11)**.
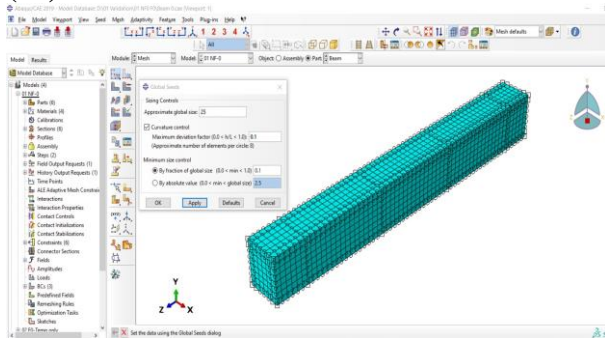
Figure 9. Meshing of Modeled Solid Beam Part.
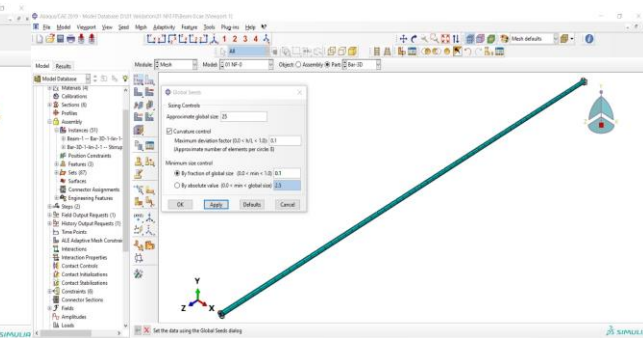
Figure 10. Meshing of Modeled Steel Main Reinforcing
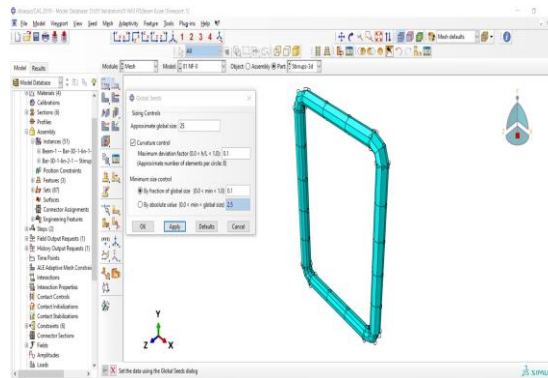
Figure 11. Meshing of the Model Steel Stirrup Reinforcing Parts.

3. NUMERICAL APPLICATIONS AND DISCUSSIONS
3.1 Numerical Module Validation

This part thoroughly investigates the suitability and significance of the considered numerical model. A numerical analysis model was adopted to simulate the behavior of burned beams. The outcomes of the numerical analysis comprising; ultimate load, load-deflection behavior, load-strain response, and crack pattern layout were all compared with those of the experimental data.

3.1.1   Ultimate Deflection and Ultimate Load Capacity.

The experimental results comprising the ultimate load and deflection are compared to that provided by the nonlinear finite element analysis (FEA) of all tested beams. The results of the ultimate load and deflection are summarized in Table (1). The experimental and FEA outcomes were in good agreement, as can be shown in Table (1). Regarding the ultimate load, the percentage of error didn't exceed (3.44) % for specimens. Moreover, the comparison shows a good agreement concerning the ultimate deflection. The percentage of error didn't exceed (6.57) % for specimens. All the percentage differences between the experimental and the numerical are acceptable. This is usually caused by the numerical analysis assumptions, in which the adopted solving process in ABAQUS software assumes full interaction between the concrete and steel rebar elements, whereas this assumption is not valid in the experimental work. **Fig. (12) to (15)**, on the other hand, provide a comparison of the experimental and numerical load-deflection curves at the specimen center.

Generally, when the numerical, analytical results are compared to the experimental work, there is a good agreement in the deflection response. The computed load-deflection curves were also found to be more uniform than the experimental load-deflection curves. This is one of the finite element analysis's considered assumptions, which assumes that the materials are homogeneous and that the concrete and steel reinforcement is completely bounded. The FEA curves showing the load-deflection response through the elastic zone are slightly stiffer than the experimental curves, as can be seen. It's worth noting that the stiffness of the tested beams is slightly lower than that of the FE models after initiating the first flexural cracks for burned specimens because the finite element modeling of the supporting lines prevented the beams from moving in both upward and downward directions, but only in the experimental set-up. In addition, handling and drying shrinkage causes micro-cracks in the concrete, lowering the stiffness of the actual beam.

Table 1. Comparison Between Experimental and FEA for Ultimate Load and Deflection.

Beam Specimens	Experimental Result		Finite Element Analysis		Ratio	
	P_u (kN)	Δ_u (mm)	P_u (kN)	Δ_u (mm)	$\left\lvert \dfrac{P_u\ Exp - P_u\ FE}{P_u\ Exp} \right\rvert \%$	$\left\lvert \dfrac{\Delta_u\ Exp - \Delta_u\ FE}{\Delta_u\ Exp} \right\rvert \%$
F-0%	100.89	22.05	97.41	23.50	3.44	6.57
F-1%	108.95	24.67	106.89	25.20	1.89	2.14
F-2%	113.90	28.31	110.83	28.78	2.69	1.66
F-3%	135.51	36.46	137.06	36.00	1.14	1.26
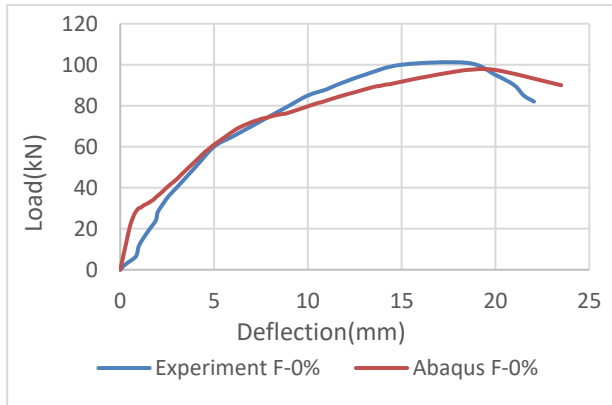
Figure 12. Experiment and Analytical Load Deflection F-0%.
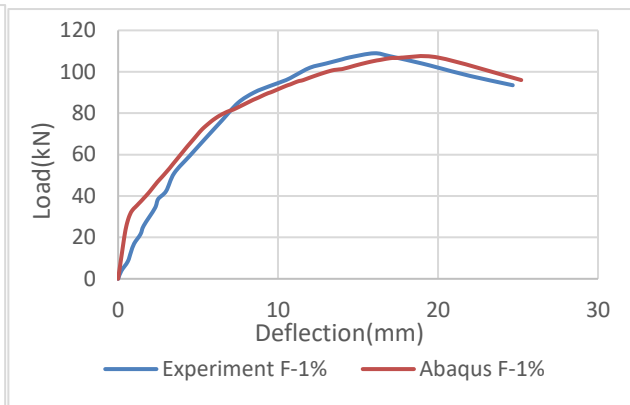
Figure 13. Experiment and Analytical Load Deflection F-1%.
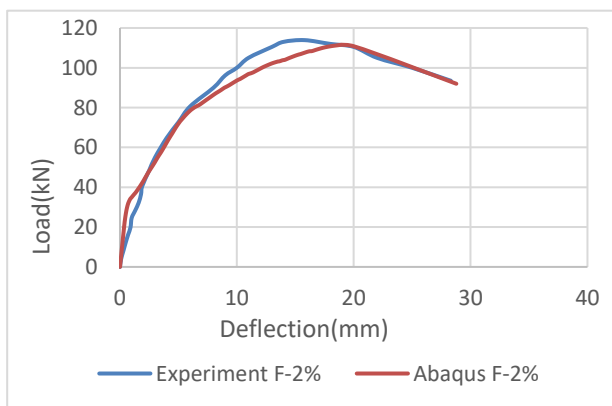
Figure 14. Experiment and Analytical Load Deflection F-2%.
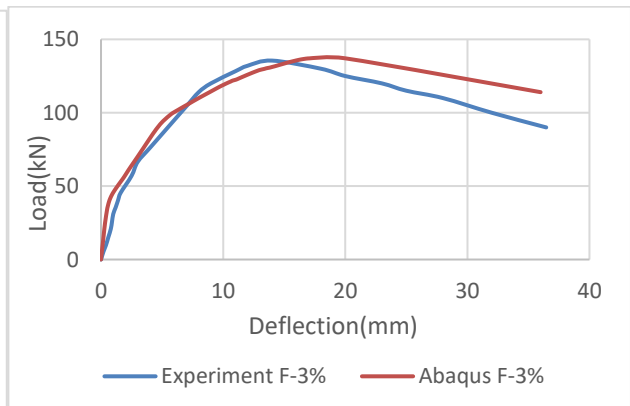
Figure 15. Experiment and Analytical Load Deflection F-3%.

3.1.2   Strain in Concrete.

Strain gauges were installed at predefined sites to measure the load-concrete strain for specimens, as shown in **Fig. (16). Table (2)** provides the experimental results as well as the ultimate numerical strain in concrete for all the tested specimens burned. The numerical results show that the experimental and the numerical results are in good agreement, the maximum difference percent reaching (1.03) % for burned specimens. The computational and experimental load-concrete strain curves are compared in **Fig. (17) to (20)**. The load-strain charts from the finite element studies match well with the experimental data for all specimens, as can be shown.

Figure 16. Locations of the Concrete Strain Gauge.

Table 2. Experimental and Numerical Ultimate Strain in the Concrete Unburned and Burned Specimens.

Specimens Designation	Experimental Strain $\times 10^{-6}$	Finite Element Strain $\times 10^{-6}$	(FEA. / EXP.)
F-0%	3575	3239	0.90
F-1%	3459	3184	0.92
F-2%	3023	2993	0.99
F-3%	2797	2881	1.03
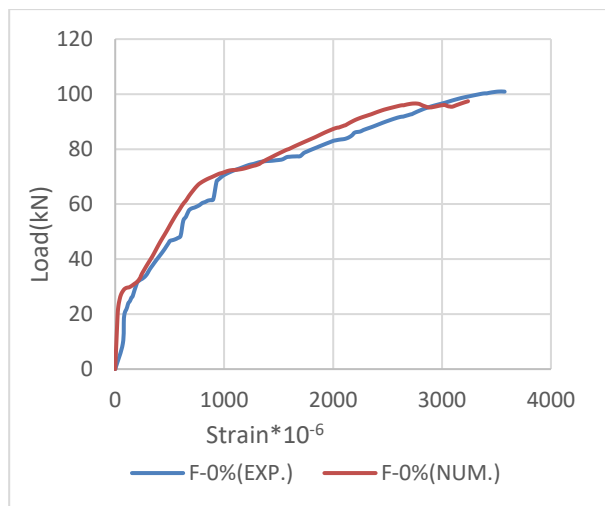
Figure 17. Load-Concrete strain curve for specimen F-0%.
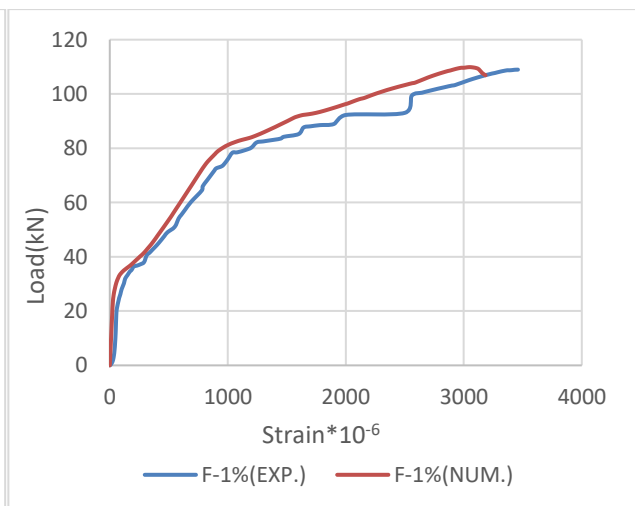
Figure 18. Load-Concrete strain curve for specimen F-1%.
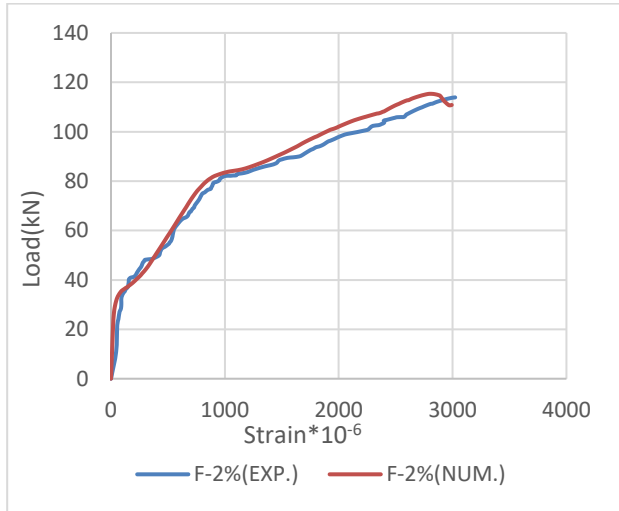
Figure 19. Load-Concrete strain curve for specimen F-2%.
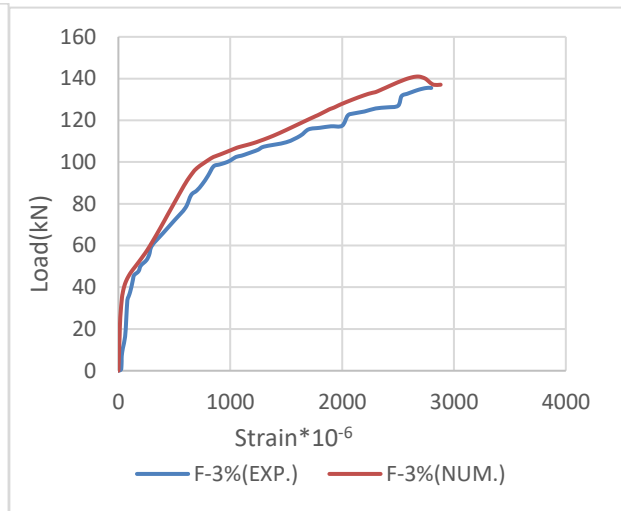
Figure 20. Load- Concrete strain curve for specimen F-3%.

3.2 Numerical Parametric Study

The influence of three steady-state burning temperatures (500, 600, and 700)℃ and burning duration (one and two) hours on the ultimate load and load-deflection response was investigated using the ABAQUS software's Finite Element Modeling. The experimental mechanical properties (compressive strength, tensile strength, and elasticity modules) of the control specimens for the concrete mixes at the adopted burning temperature (500, 600, and 700) ℃ are shown in **Table (3)**.

Table 3. Experimental Mechanical Properties for Concrete Mixes.

WAPS %	Temperature (°C)	Duration (Hour)	(f_{cu}) (MPa)	(f_t) (MPa)	E (MPa)
0%	500	1	27.79	2.50	16970.29
	600	1	20.72	1.63	15614.58
	700	1	12.50	1.03	13928.55
1%	500	1	31.70	2.73	19195.68
	600	1	23.71	1.89	16832.62
	700	1	15.23	1.21	14221.04
2%	500	1	40.56	2.92	20520.53
	600	1	28.79	2.16	18647.41
	700	1	22.42	1.63	15645.94
3%	500	1	47.06	3.31	24646.08
	600	1	36.48	2.49	21326.30
	700	1	28.46	1.98	17959.47

Concrete compressive strength for the tested cubes after burning for one hour and sudden cooling conditions showed that the compressive strength is significantly affected compared to the corresponding references (unburned). The residual compressive strength was (46.33, 50.01, 63.15, and 72.40)% at steady-state burning temperature (500℃), and (34.53, 37.40, 44.81, and 56.12)% concerning the temperature (600℃), while they were (20.83, 24.02, 34.90, and 43.78)% at temperature (700℃) for the WAPS volume ratio (0, 1, 2, and 3)%, respectively. Also, the residual splitting tensile strength for the testing cylinder of the considered WAPS volume ratio (0, 1, 2, and 3)% after a one-hour burning duration and sudden cooling process was (61.30, 65.02, 69.10, and 74.36)% for the temperature (500℃), and (39.86, 45.00, 51.31, and 56.50)% corresponding to the temperature (600℃), and (25.30, 28.91, 38.78, and 44.79)% regarding the temperature (700℃). An identical behavior was detected regarding the modulus of elasticity; the residual percentage was (66.40, 73.00, 70.00, and 75.00)% at temperature (500℃) and (61.00, 64.00, 63.00, and 65.00)% at temperature (600℃), and (54.50, 54.00, 53.00, and 55.00)% at temperature (700℃). All the outcomes of these control specimens under the considered conditions proved the enhancing effect of using WAPS on the concrete strength affected by fire flame. **Table (4)** proved the burning duration effect (one and two) hours on the concrete hardened characteristic comprising (compressive strength, splitting tensile strength, and modulus of elasticity) after using WAPS as a volume percentage. The residual compressive strength was (34.14, 22.17, 19.08, and 15.66)%. The residual splitting tensile strength for the tested cylinders after burning and cooling was (41.20, 44.32, 39.04, and 34.74)%, while the residual modules of elasticity were (12.93, 18.81, 16.59, and 20.86)% for the WAPS percentage (0, 1, 2, and 3)%, respectively, at temperature 500℃ for two hours as compared to one hour burned specimens (F-0%, F-1%, F-2%, and F-3%), respectively.

Table 4. Experimental Mechanical Properties for Concrete Mixes.

WAPS %	Temperature (℃)	Duration (Hour)	(f_{cu}) (MPa)	% Variation	(f_t) (MPa)	% Variation	E (MPa)	% Variation
	500	1	27.79	----	2.50	----	16970.29	----
0%	500	2	18.30	34.14	1.47	41.20	14775.40	12.93
	500	1	31.70	----	2.73	----	19195.68	----
1%	500	2	24.67	22.17	1.52	44.32	15583.61	18.81
	500	1	40.56	----	2.92	----	20520.53	----
2%	500	2	32.82	19.08	1.78	39.04	17114.34	16.59
	500	1	47.06	----	3.31	----	24646.08	----
3%	500	2	39.69	15.66	2.16	34.74	19503.52	20.86

4. RESULTS and DISCUSSIONS

For the burned specimens, the influence of fire flame time exposure on the ultimate load capacity and load-deflection behavior was investigated. The analysis parameters' findings showed a considerable difference in the specimens' load-carrying capability at the same burning temperature level of (500℃) when the duration of fire exposure is increased. **Table (5)** shows the percentage variation in the ultimate load and the maximum deflection for two hours duration (31.52, 34.54, 30.31, and 28.64)% and (7.32, 13.80, 16.01, and 21.00), respectively, for specimens (F-0%, F-1%, F-2%, and F-3%), respectively, with regard to the corresponding one-hour-burned specimens. The numerical findings of the ultimate load (P_u) and the maximum deflection (Δ_u) for the specimen

models at the considered burning temperatures are shown in **Table (6).** The results showed that adding WAPS as a volume ratio to the concrete mix resulted in a considerable increase in the ultimate load as well as an increase in the peak deflection as compared with the reference specimen (no WAPS contained) was achieved. **Fig. (21) to (24)** show the effect of fire exposure duration on the ultimate load, and **Fig. (25) to (28)** show the effect of steady-state temperature of the fire exposure (500, 600, and 700)°C on the ultimate load.

Table 5. Numerical Ultimate Load and Ultimate Deflection at 500℃ (two hours).

Specimen Designation	P_u (kN)	%Variation in P_u %	Δ_u (mm)	%Variation in Δ_u %	Stiffness $K=P/\Delta$ (kN/mm)
500°C(1hr.)					
F-0%	97.41	----	23.50	----	48.45
F-1%	106.89	----	25.20	----	62.00
F-2%	110.83	----	28.78	----	77.20
F-3%	137.06	----	36.00	----	96.38
500°C(2hr.)					
F-0%	66.70	31.52	25.22	7.32	20.23
F-1%	69.96	34.54	28.67	13.80	25.17
F-2%	77.24	30.31	33.39	16.01	66.70
F-3%	97.80	28.64	43.44	21.00	80.25

Table 6. Numerical Ultimate Load and Ultimate Deflection for the Considered Temperatures.

Specimen Designation	P_u (kN)	Increasing in P_u %	Δ_u (mm)	Increasing in Δ_u %	Stiffness $K=P/\Delta$ (kN/mm)
500℃					
F-0%	97.41	----	23.50	----	48.45
F-1%	106.89	9.73	25.20	7.23	62.00
F-2%	110.83	13.77	28.78	22.46	77.20
F-3%	137.06	40.70	36.00	53.19	96.38
600℃					
F-0%	69.45	----	23.67	----	13.34
F-1%	74.20	6.84	27.70	17.02	16.70
F-2%	99.80	43.70	32.13	35.74	34.75
F-3%	112.53	62.00	41.69	76.13	48.24
700℃					
F-0%	48.55	----	26.95	----	3.12
F-1%	50.50	4.00	28.57	6.01	4.17
F-2%	55.21	13.72	33.89	25.75	4.40
F-3%	68.34	40.76	45.00	66.97	6.57

Regarding the adopted parameter (steady-state burning temperature), **Table (6)** shows that the specimen with (3%) WAPS volume fraction improved the ultimate load and the ultimate deflection by about (40.70 and 53.19)%, respectively, for (500°C) and (62.00 and 76.13)%, respectively, for (600°C), and by about (40.76 and 66.97)%, respectively, for (700°C).
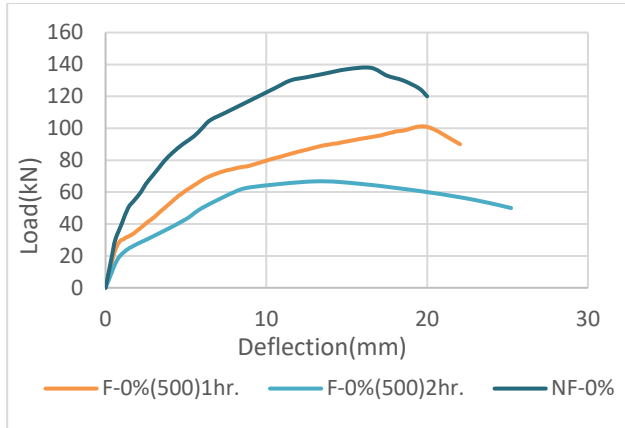
Figure 21. Effect of Fire Exposure Duration on the Ultimate Load.
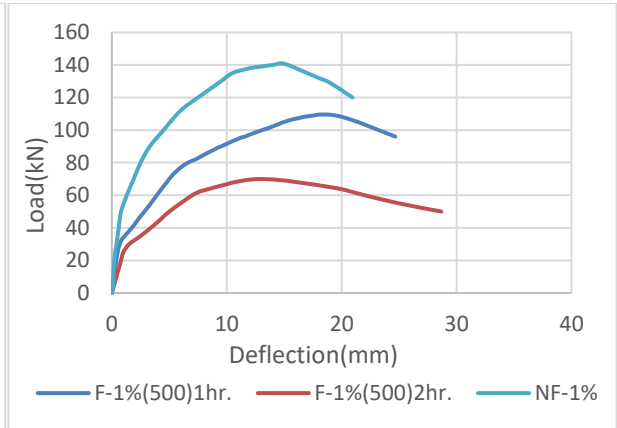
Figure 22. Effect of Fire Exposure Duration on the Ultimate Load.
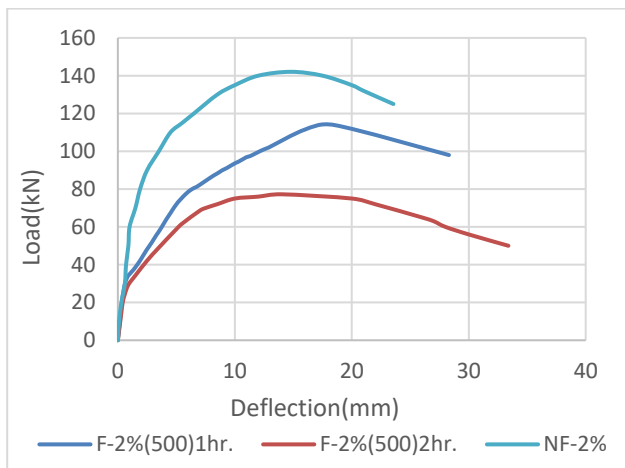
Figure 23. Effect of Fire Exposure Duration on the Ultimate Load.
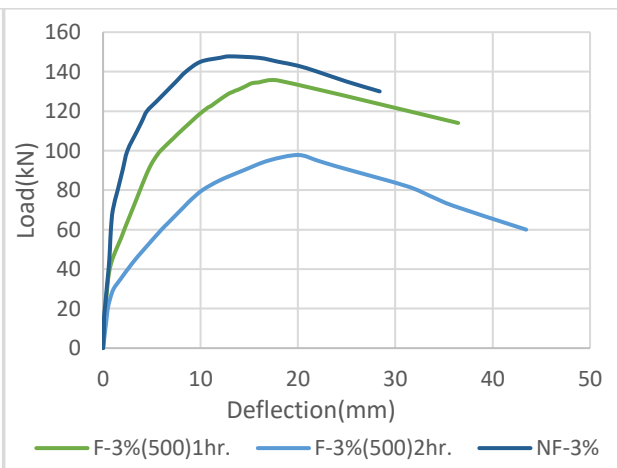
Figure 24. Effect of Fire Exposure Duration on the Ultimate Load.
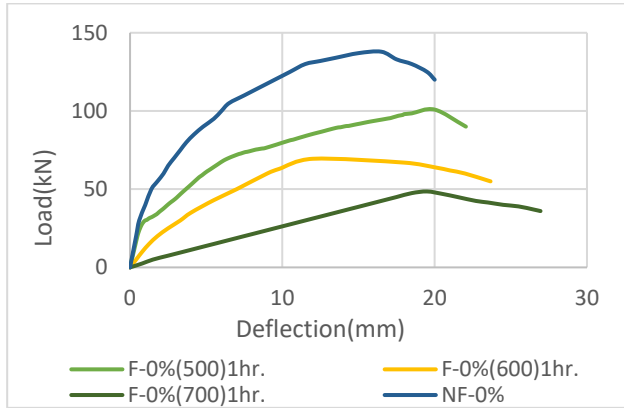
Figure 25. Effect of Fire Exposure Different Temperatures on the Ultimate Load (WAPS-0%).
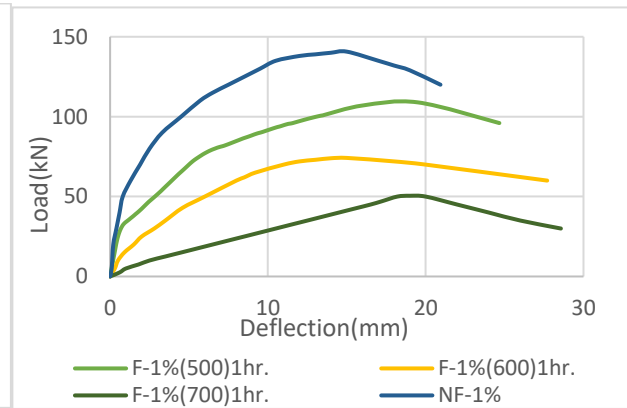
Figure 26. Effect of Fire Exposure Different Temperatures on the Ultimate Load (WAPS-1%).
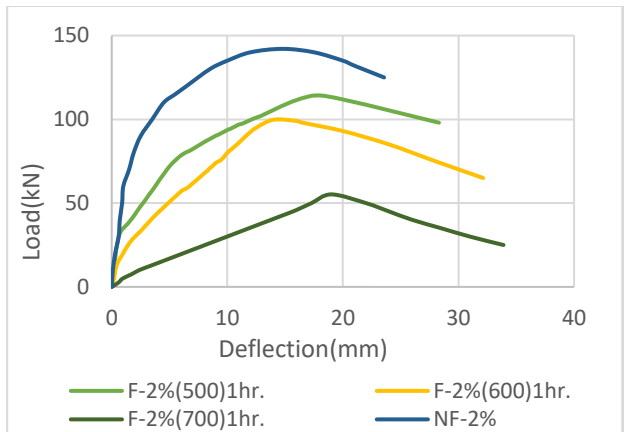
Figure 27. Effect of Fire Exposure Different Temperatures on the Ultimate Load (WAPS-2%).
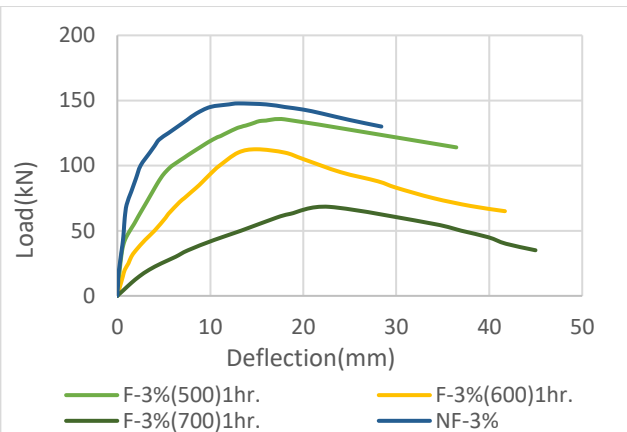
Figure 28. Effect of Fire Exposure Different Temperatures on the Ultimate Load (WAPS-3%).

The flexural toughness of reinforced concrete specimens containing various amounts of WAPS is compared in **Table (7).** Heating reduces beam stiffness, mostly due to a reduction in concrete's mechanical characteristics.

Regarding the considered parameters that included fire exposure duration (one and two hours) at (500 °C), the specimen containing a ratio (3%) of WAPS was of the best structural behavior. The percentages variation of the absorbed energy reduction at failure load were (21.39 and 37.01)% for the WAPS ratio (3 and 0)%, respectively. This proved the enhancing influence of the WAPS ratio, as shown in **Table (7).**

For the adopted parameters regarding the steady-state burning temperature (500, 600, and 700)°C for a one-hour duration, the percentages variation of the absorbed energy reduction at failure load were (91.87, 150.67, and 106.07), respectively, for specimens with a ratio of (3%) WAPS as compared with zero percentage of WAPS, as shown in **Table (8).**

Table 7. Absorbed Energy for the Burned Specimens at Temperature (500°C) for Two-Hour Duration.

Specimen Designation	Absorbed Energy at Failure Load (kN.mm)	% Variation of Absorbed Energy at Failure Load
500°C (1hr.)		
F-0%	1862.95	----
F-1%	1984.40	----
F-2%	2400.14	----
F-3%	3574.51	----
500°C (2 hr.)		
F-0%	1173.42	37.01
F-1%	1470.20	25.91
F-2%	1853.54	22.77
F-3%	2809.57	21.39

Table 8. Absorbed Energy for the Burned Specimens at Temperature (500, 600, and 700)°C for One-Hour Duration.

Specimen Designation	Absorbed Energy at Failure Load (kN.mm)	% Variation of Absorbed Energy at Failure Load
500°C (1hr.)		
F-0%	1862.95	----
F-1%	1984.40	6.52
F-2%	2400.14	28.83
F-3%	3574.51	91.87
600°C (1hr.)		
F-0%	1242.85	----
F-1%	1508.67	21.38
F-2%	2163.22	74.05
F-3%	3115.51	150.67
700°C (1hr.)		
F-0%	788.30	----
F-1%	864.85	9.71
F-2%	1121.65	42.28
F-3%	1624.52	106.07

5. CONCLUSIONS

1. Regarding the considered parameters that included fire exposure duration (one and two hours) at (500 °C), the specimen containing a ratio (3%) of WAPS was of the best structural behavior as listed in items (a - d):

a. The ultimate load was reduced by about (28.64)% due to the time duration effect while the reduction was (31.53) % for the specimen of zero WAPS.

b. The percentages variation of the absorbed energy reduction at failure load were (21.39 and 37.01) % for the WAPS ratio (3 and 0)%, respectively. This proved the enhancing influence of the WAPS ratio.

c. Regarding the burned specimen stiffness, similar outcomes were found. The reduction percentages were (16.74 and 58.25) for the WAPS ratio (3 and 0)%, respectively.

d. As for the hardening concrete properties consisting of (compressive strength, splitting tensile strength, and modulus of elasticity), the residual strengths were (15.66, 34.74, and 20.86)%, respectively, in the case of (3%) WAPS contained. In contrast, they were (34.14, 41.20, and 12.93)% in the case of (0%) WAPS.

2. For the adopted parameters regarding the steady-state burning temperature (500, 600, and 700)$^\circ$C for a one-hour duration, the specimens with a ratio of (3%) WAPS improved the following, corresponding to zero percentage of WAPS:

a. Has the highest ultimate load and the ultimate deflection by about (40.70 and 53.19)%, and (62.00 and 76.13)%, and by about (40.76 and 66.97)%, respectively.

b. The absorbed energy at failure load by about (3574.51, 3115.51, and 1624.52) kN.mm.

c. The stiffness by about (96.38, 48.24, and 6.57) kN/mm

d. The residual compressive strength, splitting tensile strength, and modulus of elasticity were (72.40, 56.12, and 43.78)%, (74.36, 56.50, and 44.79)%, and (45.23, 36.57, and 28.94)%, respectively.

REFERENCES

ABAQUS Standard user's manual, Volumes I-III, Version 6.8. Pawtucket (America): Hibbitt, Karlsson & Sorensen, Inc.; 2008.

Abaqus Analysis User's Guide Volume IV: Elements. Waltham, MA, USA: Dassault Systems, 2014.

D. L. Logan, 2012. *A first course in the FE method, fifth edition.* United States of America: Global Engineering: Christopher M. Shortt.

Eurocode 2, 2004. Design of concrete structures, Part 1-2: General rules -Structural fire design *Euro code SS-EN-1992-1-1:2008*, 3(July).

Eurocode 3, 2011. Design of steel structures, Part 1-1: General rules and rules for buildings, EN-1993-1-1:2011. March 2009

Eurocode 4., 2005. Design of composite steel and concrete structures– 'EN 1994.Part 1-2: General rules - Structural fire design, (August), pp. 1-109.

Amer F. Izzat, Jamal A. Farhan, and Ammar A. Hammadi. Effect of Fire Flame (High Temperature) on the Self Compacted Concrete (SCC) One Way Slabs, *Journal of Engineering*, Collage of Engineering, University of Baghdad, (2012): 1083-1099.

Amer F. Izzat, 2015. Retrofitting of Reinforced Concrete Damaged Short Column Exposed to High Temperature, *Journal of Engineering*, Collage of Engineering, University of Baghdad.

El-Tayeb, E. H., El-Metwally, S. E., Askar, H. S., and Yousef, A. M., 2017. Thermal analysis of reinforced concrete beams and frames, *HBRC Journal*, 132 Housing and Building National Research Center, 13(1), pp. 8–24.

Gao, W. Y., Chen, G. M., Teng, G. J., and Dai, J. G., 2013. Finite element modeling of reinforced concrete beams exposed to fire. Elsevier Ltd, 52, pp. 488–501. DOI: 10.1016/j.engstruct.2013.03.017.

"Getting Started with Abaqus: Interactive Edition (6.10)," Abacus 6.10. http://130.149.89.49:2080/v6.10/books/gsa/default.htm?startat=ch01s02.HTML (accessed Dec. 20, 2020).

ISO 834-1, 1999. Fire Resistance Tests-Elements of Building Construction. Part 1: General Requirement, International Organization for Standardization, Geneva, Switzerland.

N.-H. Kim, 2014. Introduction to Nonlinear Finite Element Analysis. New York, NY, USA: Springer.

Ozˇbolt, J., Bošnjak, J., and Periškic, A. S., 2013. 3D numerical analysis of reinforced concrete beams exposed to elevated temperature, *Engineering Structures (2013)*, pp. 1–9.

Yue, M.G., Yao, Q.L., Wang, Y.Y., and Li, H.N., 2008. Numerical Simulation on The Fire Proof Behavior of RC Beams with Strand Mesh and Polymer Mortar-The 14World Conference on Earthquake Engineering October 12-17, Beijing, China, PP. 1-6.